Ionization and recombination in attosecond electric field pulses

Darko Dimitrovski,[1,2] Eugene A. Solov'ev,[2] and John S. Briggs[1]
[1]*Theoretische Quantendynamik, Universität Freiburg, Hermann-Herder-Strasse 3, D-79104 Freiburg, Germany*
[2]*Macedonian Academy of Sciences and Arts, 1000 Skopje, Macedonia*
(Received 2 February 2005; published 31 October 2005)

Based on the results of a previous communication [Dimitrovski *et al.*, Phys. Rev. Lett. **93**, 083003 (2004)], we study ionization and excitation of a hydrogenic atom from the ground and first excited states in short electric field pulses of several cycles. A process of ionization and recombination which occurs periodically in time is identified, for both small and extremely large peak electric field strengths. In the limit of large electric peak fields closed-form analytic expressions for the population of the initial state after single- and few-cycle pulses are derived. These formulas, strictly valid for asymptotically large momentum transfer from the field, give excellent agreement with fully numerical calculations for all momentum transfers.

DOI: 10.1103/PhysRevA.72.043411 PACS number(s): 42.50.Hz, 32.80.Fb, 34.90.+q

I. INTRODUCTION

The observation and control of quantum phenomena in atoms and molecules using newly developed laser techniques is an area of great current interest [1]. In particular, the development of attosecond (more accurately "a fraction of a femtosecond") pulses has been rapid in recent years [2–6]. Presently, the free-electron laser source at DESY produces pulses with frequency ~ 0.5 a.u., total pulse duration 50 fs, and intensities up to 7×10^{13} W/cm^2 (corresponding to a peak electric field of ~ 0.044 a.u.) [2,3][1], whereas the high-frequency laser pulses produced from a high-harmonic generation have a frequency around $\omega=3.3$ a.u. and minimal duration of 0.65 fs [4] and recently of 0.25 fs [6]. In both cases, the envelopes of the pulses produced are not well controlled and each pulse contains more than five (in the DESY case more than 100) cycles. Very recently a train of almost single-cycle pulses of duration 0.17 fs has been realized [7]. A truly few-cycle pulse has been produced for frequency $\omega \approx 0.05$ a.u. [8]. The attosecond few-cycle pulse awaits the development of attosecond high-power lasers with controllable pulse envelopes, but since progress in laser physics is explosive, there is reason to hope that such lasers will be available in the near future. Alternatively one can use relativistic time dilatation to obtain short, very strong field pulses in the frame of target particles moving at relativistic velocities, although here one is restricted to ions in storage rings.

There has been an enormous amount of theoretical work on the ionization of atoms by strong lasers. However, in the early days, this was mostly confined to the cw laser regime. The observation of real-time electronic processes requires extremely short pulses where only a few cycles (in fact down to a half cycle) of the electromagnetic field occur in the pulse duration. This opens up a completely new area for theory. Most of the theoretical approaches for studying several-cycle pulses employed so far are wholly numerical, except for a small number of analytic results based on the Keldysh-Faisal-Reiss approximation [9,10] and Coulomb-Volkov approach [11]. Here we will consider the situation where the oscillation period is short compared to the orbital time in the initial state. In this regime there are a large number of papers concerning ionization of Rydberg states (see for example [12–14]) including purely analytic nonperturbative studies of Rydberg atom excitation and ionization for the case of half-cycle pulses [15–17]. However, for few-cycle pulses, so far the theoretical approaches have been limited to numerical studies only.

In a previous Letter [18], to be referred to as paper I, we studied the ionization of the ground-state hydrogen atom in a short half- or single-cycle electric field pulse. Here we present more extensive results and in particular generalize the strong-field case to several-cycle pulses and to ionization from excited states of the hydrogen atom. In addition we study the energy and particularly angular distributions of ionized electrons. The conclusion of I, that for pulse periods less than an orbital period a process like Rabi flopping on the continuum can occur, is reinforced by the results presented here. In this way, using suitably designed pulses, a control of the continuum occupation probability (or correspondingly that of the initial state) can be achieved. Throughout we use atomic units.

II. THEORY

For an initial state $\Phi_i(t_0)$ we calculate the time propagation to time t, i.e.,

$$|\Psi_i(t)\rangle = U(t,t_0)|\Phi_i(t_0)\rangle \tag{1}$$

where the time-development operator is defined by

$$H(t)U(t,t_0) = i\,\partial U/\partial t \tag{2}$$

with, in dipole approximation,

$$H(t) = H_0 + \mathbf{r}\cdot\mathbf{F}(t) \equiv H_0 + V(t). \tag{3}$$

Here H_0 is the atomic Hamiltonian and $\mathbf{F}(t)$ describes the magnitude (whose peak value we denote by F_0) and polarization of the classical electric field.

The probability amplitude of occupation of any final state is then simply

[1]For electric field strength 1 a.u.$=5.1423\times 10^9$ V/cm.

$$a_{fi}(t) = \langle \Phi_f(t) | \Psi_i(t) \rangle \tag{4}$$

and the corresponding probability is $P_{fi}(t) = |a_{fi}(t)|^2$.

The most accurate method of calculating $\Psi_i(t)$ from Eq. (1) is to propagate the initial wave function in time according to the time-dependent Schrödinger equation (TDSE)

$$H(t)|\Psi_i(t)\rangle = i\frac{\partial}{\partial t}|\Psi_i(t)\rangle \tag{5}$$

obtained by applying (2) on $|\Phi_i(t_0)\rangle$. This we have achieved by propagating the wave function, completely numerically with no approximations, on a three-dimensional grid using the discrete-variable representation (DVR) method. The details of this numerical approach are given in Ref. [19]. As with all fully numerical approaches, the results provide little insight into the physics underlying the time development. Therefore we examine two limits where analytical solutions are possible. The first is standard first-order perturbation approximation (FPA), valid when $F_0 \ll 1$ a.u. Here we give closed forms for N-cycle rectangular and sinusoidal pulses. Remarkably, the physics of ionization by very intense pulses ($F_0 > 1$ a.u) becomes rather simple and, somewhat unusual in strong-field laser-atom interactions, we can give analytic expressions for excitation and ionization probabilities so long as the half-cycle duration is less than the initial orbital period. These expressions are obtained using the first Magnus approximation (FMA) to the exact propagator defined in Eq. (2). By modifying the FMA to allow for propagation of the ionized electron in the nuclear Coulomb field, we can even obtain analytic expressions for the ionization probability after N-cycle pulses.

The time propagator in Eq. (2) is defined formally also by the integral equation

$$U(t,t') = U_0(t,t') - i\int_{t'}^{t} U_0(t,t'')V(t'')U(t'',t')dt'' \tag{6}$$

where $U_0(t,t') = \exp[-iH_0(t-t')]$ is the propagator of the atomic field alone. In first-order perturbation theory one replaces U on the right-hand side of Eq. (6) by U_0 and substitutes in Eqs. (1) and (4) to give

$$a_{fi}(t) = \langle \Phi_f(t)|U_0(t,t_0)|\Phi_i(t_0)\rangle - i\int_{t_0}^{t} \langle \Phi_f(t)|U_0(t,t')V(t')U_0(t',t_0)|\Phi_i(t_0)\rangle dt'. \tag{7}$$

If $\Phi_i(t_0) = \phi_i \exp(-iE_i t_0)$ and $\Phi_f(t) = \phi_f \exp(-iE_f t)$, where ϕ_i and ϕ_f are eigenstates of H_0 with different eigenvalues E_i and E_f, then the first term in Eq. (7) is zero and one obtains

$$a_{fi}(t) = -i\int_{t_0}^{t} \langle \phi_f|V(t')|\phi_i\rangle \exp[i(E_f - E_i)t']dt', \tag{8}$$

which is the standard first-order perturbation result.

For intense pulses, in general when the electric field is bigger than the atomic field potential, the perturbation theory does not converge. However, if the pulse time is very short one can employ an approximation to $U(t,t')$ first suggested by Magnus [20] and considered in detail by Pechukas and Light [21]. If H and U commute, Eq. (2) can be integrated to yield

$$U(t,t_0) = \exp\left(-i\int_{t_0}^{t} H(t')dt'\right). \tag{9}$$

However, this is not possible since $H(t_1)$ and $H(t_2)$ do not commute for any two times t_1 and t_2. Nevertheless, the Magnus expansion shows that, for small $(t-t_0)$, Eq. (9) can be used as the first approximation to $U(t,t')$ the corrections involving, as one might expect, the nested commutators of $H(t)$ at different times. Then if one makes the further assumption that $V(t)$ is short compared to the orbital times of eigenstates of H_0, one can neglect the noncommutativity of H_0 and $V(t)$ to write

$$\begin{aligned} |\Psi_i\rangle &= U(t,t_0)|\Phi_i(t_0)\rangle \\ &\approx \exp\left(-i\int_{t_0}^{t} V(t')dt'\right)\exp[-iH_0(t-t_0)]|\Phi_i(t_0)\rangle \\ &= \exp\left[-i\left(\int_{t_0}^{t} \mathbf{F}(t')dt'\right)\cdot\mathbf{r}\right]\exp(-iE_i t)|\phi_i\rangle. \end{aligned} \tag{10}$$

Then, defining

$$\mathbf{q} = \int_{t_0}^{t} \mathbf{F}(t')dt' \tag{11}$$

as a momentum boost, one has the simple result

$$P_{fi} = |\langle \phi_f|\exp(-i\mathbf{q}\cdot\mathbf{r})|\phi_i\rangle|^2, \tag{12}$$

which we will call the FMA.

One remarks here on the close analogy between the FMA for short light pulses and excitation and ionization by the electric fields of charged particles. For electron or heavy-ion impact in the first Born approximation, the transition matrix element is exactly that appearing in Eq. (12), where $\mathbf{q}$ is then the change in momentum of the projectile, or equivalently the momentum transferred to the target atom. For heavy ions moving at velocities high enough that their motion can be described by a classical trajectory the analogy is even closer. Then, for distant collisions where the dipole term of the Coulomb force is dominant, the transition matrix element is again of the form (12) in the FMA, with the momentum transfer $\mathbf{q}(t)$ given exactly as in Eq. (11) by an integral over the electric field of the incident heavy ion. When the momentum transfer becomes small so that $e^{-i\mathbf{q}\cdot\mathbf{r}} \approx 1 - i\mathbf{q}\cdot\mathbf{r}$, the FMA transition amplitude becomes

$$a_{fi} \approx -i\mathbf{q}\cdot\langle \phi_f|\mathbf{r}|\phi_i\rangle. \tag{13}$$

Similarly when $(E_f - E_i)\tau \ll 1$, i.e., for a short pulse the expression (8) in the first-order perturbation approximation reduces to Eq. (13). Hence, the FMA and FPA give identical results for short, weak pulses. The FPA remains valid for long, weak pulses, the FMA for short, stronger pulses. The expression (13), following Ref. [22], will be referred to as the sudden approximation (SA).

In the context of a study of sudden perturbations, the FMA (12) has also been derived by Dykhne and Yudin [23] who referred to it as the "jarring" or "shakeup" approximation, presumably since they applied it to atomic excitation resulting from a sudden change in the nuclear potential (e.g., as in neutron scattering). Subsequently this shakeup approximation has been applied many times to laser-atom interactions (see, e.g., [24,25]). However, in our case the momentum transfer is directly to the atomic electron as in charged-particle impact and the description "shakeup" is not exactly appropriate. Hence we prefer to emphasize the analogy to charged-particle impact and refer to Eqs. (11) and (12) as the first Magnus approximation.

III. FIRST-ORDER PERTURBATION THEORY

The FPA is normally applied to situations where the pulse contains an enormous number of cycles, e.g., cw laser ionization. Then one obtains a constant ionization rate known as Fermi's golden rule. In this case the ejected electrons are monochromatic, corresponding to the absorption of a single photon from the ground state. However, for short pulses in time, as one might expect from elementary considerations of the time-to-energy Fourier transform embodied in Eq. (8), the spectrum of ejected electrons exhibits considerable structure extending over an extremely wide energy range, as shown by the initial results reported in I.

As an example we consider specifically a pulse consisting of a train of m alternating half cycles each of duration τ and of either rectangular or sinusoidal form. The ionization probability from the ground state ϕ_1, with binding energy $|E_1|$, to a final state $\phi_{\mathbf{k}}$ of momentum $\mathbf{k}$, integrated over all angles of emission, is given by

$$\frac{dP}{dE} = k \int d\hat{\mathbf{k}} |a(\mathbf{k})|^2 \tag{14}$$

where

$$a(\mathbf{k}) = -i \int_0^{m\tau} \mathbf{F}(t) \cdot \langle \phi_{\mathbf{k}} | \mathbf{r} | \phi_1 \rangle \exp(i\epsilon t) dt,$$

$$\epsilon = E - E_1 \quad \text{and} \quad E = \frac{k^2}{2}.$$

This time integral can be performed to give

$$\frac{dP}{dE} = F_0^2 u_1(E) \left| \frac{[1-\exp(i\epsilon\tau)][1-(-1)^m \exp(i\epsilon m\tau)]}{\epsilon[1+\exp(i\epsilon\tau)]} \right|^2$$

$$= 4F_0^2 u_1(E) \frac{\sin^2\left(\frac{1}{2}\epsilon\tau\right)\sin^2\left[\frac{1}{2}(\epsilon - \pi/\tau)m\tau\right]}{\cos^2\left(\frac{1}{2}\epsilon\tau\right)\epsilon^2} \tag{15}$$

for a sequence of rectangular pulses of magnitude F_0 and duration τ. Here we defined the function

$$u_1(E) = k \int |\langle \phi_{\mathbf{k}} | \mathbf{r} | \phi_1 \rangle|^2 d\hat{\mathbf{k}}.$$

For a sequence of sinusoidal pulses, i.e., $F(t) = F_0 \sin(\pi t/\tau)$ and $0 < t < m\tau$, one obtains

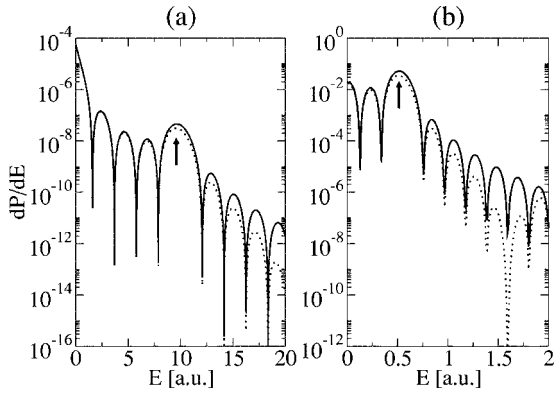

FIG. 1. The energy distribution of ionized electrons for ten half cycles of duration (a) $\tau = 0.3$ a.u., $q = 9 \times 10^{-3}$ a.u. and (b) $\tau = 3$ a.u., $q = 0.09$ a.u., calculated from Eqs. (15) and (16).

$$\frac{dP}{dE} = \left(\frac{F_0\pi}{\tau}\right)^2 u_1(E) \left| \frac{[1-(-1)^m \exp(i\epsilon m\tau)]}{\epsilon^2 - (\pi/\tau)^2} \right|^2$$

$$= 4\left(\frac{F_0\pi}{\tau}\right)^2 u_1(E) \frac{\sin^2 \frac{1}{2}(\epsilon - \pi/\tau)m\tau}{[\epsilon^2 - (\pi/\tau)^2]^2}. \tag{16}$$

The energy distributions resulting from five full-cycle pulses are shown in Fig. 1 of paper I. For $\tau = 0.3$ a.u. the energy distributions peak strongly at zero energy and show considerable structure. For sinusoidal pulses the harmonic peaks decrease smoothly as a function of energy whereas for square pulses the harmonics are folded with the $\{\sin[\frac{1}{2}(E - E_1)\tau]/\frac{1}{2}(E-E_1)\tau\}^2$ Fourier transform of a single half cycle and the higher-energy part of the distribution shows peaks at $E_1 + \omega_0 + \omega_0(1+2j)/m$, $j \geq 1$. This behavior is illustrated further in Fig. 1 of this paper where we concentrate attention on the low-energy part of the electron emission spectrum, again for five-cycle pulses of rectangular or sinusoidal form. The rectangular pulse has field strength F_0 and the peak of the sinusoidal pulse is shown as $\pi F_0/2$ so q is the same in both cases. Then one sees that near threshold dP/dE is independent of pulse shape but differences appear at higher energies due to the differences in the Fourier transforms of the pulses, as detailed above. The energy distributions also show a broad peak, indicated by arrows on Fig. 1, near $E = \pi/\tau$, which corresponds to the frequency of oscillation of the pulses. For $\tau = 0.3$ a.u. this peak is much smaller than the $E = 0$ emission probability. However, for longer pulses, for example, for ten half cycles with $\tau = 3$ a.u., corresponding to total pulse time of 30 a.u. [Fig. 1(b)], this peak grows and dominates the emission of zero-energy electrons. Of course this is just the onset of the behavior appropriate to an infinitely long pulse, where this resonance peak becomes a δ function corresponding to one-photon absorption with $E = \pi/\tau + E_1$.

In Fig. 2 of paper I, it was shown that for the region of lower-energy electron emission (≤ 2 a.u.) dP/dE exhibits an oscillatory behavior as a function of time, in that the ionization caused by a unidirectional rectangular half-cycle pulse is drastically reduced by a subsequent half cycle of opposite direction. Adding a third half cycle results essentially in the restoration of the ionization probability for one half cycle. To

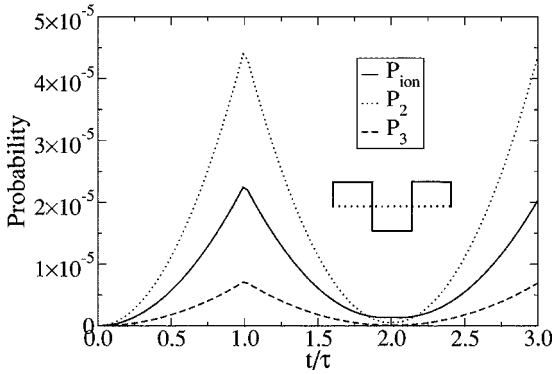

FIG. 2. The excitation probability P_n (of the nth shell, $n=2,3$) and the ionization probability P_{ion} for a rectangular pulse with $F_0=0.03$ a.u. and $\tau=0.3$ a.u. as functions of time. The probability of population of the other bound shells with $n>3$ is negligibly small.

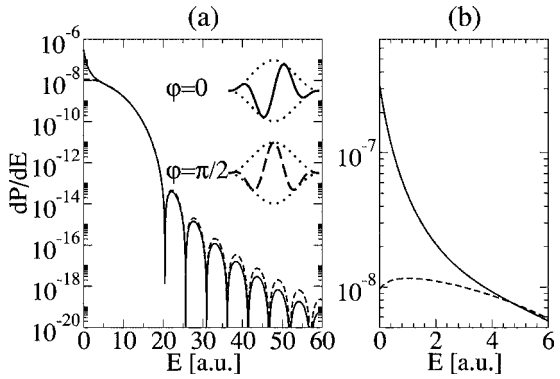

FIG. 3. Energy distribution of continuum electrons for a two-cycle laser pulse with $\tau=0.3$ a.u. and $q=9\times10^{-3}$ a.u. and an assumed $\sin^2$ envelope for the $\phi=0$ and $\pi/2$ cases.

our knowledge, that this oscillation of ionization and recombination occurs even in the perturbative regime has not been pointed out before. In Fig. 2 this behavior is made explicit by plotting the time-dependent occupation probability of the continuum (dP/dE integrated over all E) and of the $n=2$ and 3 shells, during a three-half-cycle pulse. Although the absolute probabilities are low, one notes that ionization is as probable as excitation and that all probabilities oscillate so that at $t=2\tau$, a one-cycle pulse, almost all probability has returned to the ground state. Note that in dipole approximation from the ground state only p states ($l=1$) are populated, so that the angular distribution is purely $\cos^2\theta$.

The origin of the recombination is simply due to the quantum phase reversal which arises from reversing the electric field. Classically one could view the polarization (ionization) caused by the first half cycle as simply being reversed by switching the electric field direction in the second half cycle. The small residual ionization is just due to the high-momentum components of the ionized wave packet which leave the interaction region quickly enough to avoid recombination.

A further interesting effect in the perturbation regime is the strong dependence of the ionization probability on the phase of the electric field. We consider a two-cycle ($m=4$) sinusoidal pulse with a $\sin^2$ envelope, i.e.,

$$F(t)=F_0\sin^2(\pi t/4\tau)\sin(\pi t/\tau+\phi),\quad t\in[0,4\tau], \quad (17)$$

where ϕ is the relative phase of envelope and carrier. The pulse forms for $\phi=0$ and $\pi/2$ are shown in Fig. 3(a). The choice (17) ensures that $F(t)$ does not have a dc component so that the time integral over the pulse yields zero. From Fig. 3(a) the shape of dP/dE, obtained in the FPA, is largely independent of ϕ, since it is decided essentially by the carrier envelope. However the magnitude of ionization is very sensitive to ϕ and in particular, as shown in Fig. 3(b), where the low-energy part of the spectrum is magnified, one sees that a phase change of $\pi/2$ brings more than one order of magnitude change in the ionization probability near threshold.

IV. THE STRONG-FIELD SHORT-PULSE CASE

When τ is shorter than the initial-state orbital time but q (i.e., F_0) is large, then the FMA of Eqs. (11) and (12) is appropriate. One notes that in this approximation only the integral over the pulse duration appears corresponding to the momentum boost $\mathbf{q}$ given by Eq. (11). For a single half-cycle rectangular pulse $\mathbf{q}=\mathbf{F}_0\tau$ and for a single half-cycle sinusoidal pulse $\mathbf{q}=2\mathbf{F}_0\tau/\pi$. However, the value of $\mathbf{q}$ is independent of pulse shape and one can replace $\mathbf{F}(t)$ by a δ pulse, i.e.,

$$\mathbf{F}(t)=\mathbf{q}\delta(t-t_1),\quad t_1\in(0,\tau). \quad (18)$$

The validity of this was demonstrated explicitly in I, where the FMA result was compared to exact numerical DVR results for rectangular and sinusoidal pulses (Fig. 3 of that paper). Since, for hydrogenic atoms, the matrix elements of the momentum boost operator are known in closed form [26–28], the ionization probability (12) can be calculated analytically. This is somewhat unusual in the strong-field case where often, even in numerical work, the approximation of reduced dimensionality or cutoff Coulomb potentials has been made.

Initially we consider a single short pulse and examine the momentum spectra of ionized electrons as a function of $\mathbf{q}$. In particular we see where the sudden approximation (13) is valid. In Fig. 4, we show dP/dE for four values of q. On the insets of the same figure we show angular distributions given by

$$A(\hat{\mathbf{k}})=\int|a(\mathbf{k})|^2dk.$$

When $q\ll1$ a.u. in Fig. 4(a), one sees that for dP/dE the FMA and its dipole limit the SA agree perfectly. For the same case the agreement of the FMA angular distribution (shown on the inset) and the expected p-wave angular distribution in the dipole limit is not so good. The angular distribution in the dipole limit has forward-backward symmetry even though the field is unidirectional [29], and as can be seen from Fig. 4(a) the FMA result is not perfectly forward-backward symmetrical although q is very small. This indicates that the angular distribution is a more sensitive test of

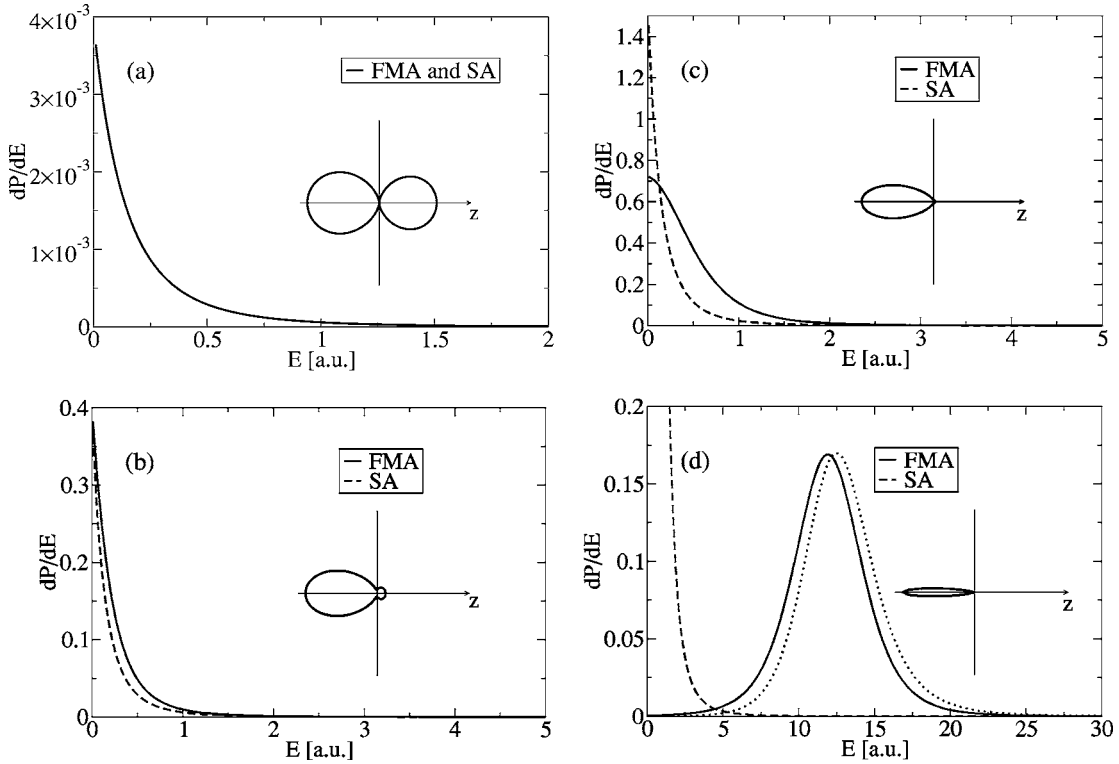

FIG. 4. Energy distributions obtained after one short pulse ($\tau \ll 1$ a.u.) for q= (a) 0.05, (b) 0.5, (c) 1, and (d) 5 a.u. in the FMA and in the SA. The dotted line in the case (d) is the energy distribution obtained by projection on plane waves. The insets show the angular distribution with respect to the field z direction.

approximations than the energy distribution. As q is increased the SA breaks down as can be seen already for $q=0.5$ a.u. in Fig. 4(b), the angular distribution becoming directed strongly along the field. The dipole contribution of the SA remains peaked at zero emission energy but the FMA gradually acquires a peak near to $E=q^2/2-|E_i|$ as q becomes large. This is the binary peak, well known in collision physics, corresponding to the initially bound electron receiving all the transferred momentum, with the nucleus acting as a spectator. This simple physical picture is illustrated best in momentum space. The distribution of the initial momentum of the bound electron is given by the momentum-space wave function $\tilde{\phi}_i(\mathbf{p})$, i.e., for a $1s$ electron in a field of a nucleus of charge Z

$$|\tilde{\phi}_i(\mathbf{p})|^2 = \frac{(2Z)^5}{4\pi^2}\frac{1}{(p^2+Z^2)^4}. \tag{19}$$

For a large ejected momentum $\mathbf{k}$ it is sufficient to replace the continuum Coulomb wave by a plane wave so that Eq. (12) becomes

$$P_{fi} = |\tilde{\phi}_i(\mathbf{q}+\mathbf{k})|^2 = \frac{(2Z)^5}{4\pi^2}\frac{1}{(|\mathbf{q}+\mathbf{k}|^2+Z^2)^4}. \tag{20}$$

Hence one sees that the initial momentum distribution, centered around momentum $p=0$ from Eq. (19), is simply lifted, without change of shape, to be centered around $\mathbf{k}=-\mathbf{q}$ with corresponding energy shift $q^2/2+|E_i|$. One also sees from Eq. (20) that the energy distribution peaks near $k=q$ ($E=q^2/2$) as shown in Fig. 4(d). On the same figure the dotted line, denoted as projection on the plane waves, is the energy distribution according to Eq. (20). Indeed, as $q\to\infty$ the distribution (20) is proportional to $\delta(\mathbf{q}+\mathbf{k})$ expressing the binary condition. From Eq. (20) the qualitative features of the small-q energy distributions are also established. The distribution (19) has a width $\langle p\rangle \sim Z$ so that for $q<Z$, the peak of the distribution is not shifted appreciably and the equivalent energy shift $q^2/2$ is less than the binding energy $|E_1|=Z^2/2$. Hence only the tail of the distribution (20) is evident at positive energies, i.e., the distribution peaks at $E=0$ as in Fig. 4(a). By contrast for $q \gg Z$ (=1 for hydrogen), as in Fig. 4(d), the whole distribution, peaked at the binary condition $k=q$, is evident.

Such a "binary collision" interpretation of energy distributions has already been suggested in Refs. [11] and [17]. In the latter reference it was also clearly pointed out that a pure half-cycle pulse cannot be realized in practice, since the total time integral over the pulse must be zero. From Eqs. (11) and (12) this would appear to imply that the FMA always yields zero ionization. However, this is not necessarily so. For example in Ref. [12] it is shown that pulses can be created with an initial short large-amplitude half cycle followed by a much weaker and much longer half cycle in the opposite direction (see Fig. 1 of Ref. [12]). Hence, on the first half cycle the initial momentum "kick" is described by the FMA correctly. The second half of the pulse does not appreciably change the total ionization probability but may distort the measured momentum distribution somewhat. Quite how the distributions of Fig. 4 will be changed will depend on details

of each particular experiment. Distortions can be minimized, either by accelerating the electrons out of the pulse region by a static electric field or by suitably focusing the pulse so that energetic electrons escape the effect. For these reasons one should not necessarily view the results of Fig. 4 as representing distributions measurable in a real experiment. Rather they should be considered as a "snapshot" of the state of the electron taken at the half-cycle pulse time. This helps to understand the subsequent behavior of the ionization process in the N-cycle pulses to be considered below.

N-cycle case

In the FMA, an even number of half cycles with the same amplitude results, at the end of the pulse, in no ionization and excitation at all, i.e., it appears that *nothing has happened*. However, the numerical results show that this is not the case. Therefore, we have modified the FMA to allow propagation in the Coulomb field of the nucleus between the half cycles. To illustrate this point precisely, in the case of a single-cycle pulse one approximates the influence of one cycle by two alternating δ pulses, each of them with an amplitude equal to the momentum transfer of a half cycle as defined in Eq. (18), and a time shift between the δ pulses equal to a half-cycle duration [illustrated in Fig. 9(b)]. Here one should mention two points. First, although this modified FMA is formally similar to the numerical split-operator method [30] we use only *one* δ function per half cycle, the use of a δ function meaning that in the moment of interaction the Coulomb field is neglected. The second point concerns the short interaction time which is crucial for the validity of our modified FMA. Because of the short interaction time, the electronic wave function does not have time to move away from the Coulomb center and therefore the electron must be described by Coulomb waves, i.e., approximating the continuum eigenstates as plane waves is inappropriate. Such an intuitive approximation of the sinusoidal time dependence of the pulse by a train of alternating δ pulses has been already considered in a purely numerical study [31] where qualitative features of ionization from a soft-core potential for pulses of around 50 cycles were considered.

In the modified FMA, N cycles are equivalent to a sequence of $2N$ δ pulses of alternating sign separated by the half-cycle time τ, i.e.,

$$F(t) \approx F_N(t) = q \sum_{j=0}^{2N-1} (-1)^j \delta(t - j\tau). \tag{21}$$

In this case the transition amplitude becomes

$$a_{fi}(N) = \langle \phi_f | e^{i\mathbf{q}\cdot\mathbf{r}} e^{-i\hat{H}_0\tau} (e^{-i\mathbf{q}\cdot\mathbf{r}} e^{-i\hat{H}_0\tau} e^{i\mathbf{q}\cdot\mathbf{r}} e^{-i\hat{H}_0\tau})^{N-1} e^{-i\mathbf{q}\cdot\mathbf{r}} | \phi_i \rangle. \tag{22}$$

The case of a single half-cycle pulse [$N=1/2$ in Eq. (21)] was considered in I where it was shown that for $\tau=0.3$ a.u. and $q>3$ a.u. all the population of the ground state is transferred to the continuum (Fig. 4 of paper I). In fact the situation is a little more subtle than shown in paper I. From Fig. 5(a) one sees that for $q>3$ a.u. all atoms are ionized after the pulse (the FMA result agrees perfectly with the DVR results in this case). As a function of q the depopulation of the ground state is continuous and monotonic. However, the population of the $n \geqslant 2$ shell shown in Fig. 5(b) first increases with q and then decreases to zero. The probability of excitation of the nth shell from the ground state in the FMA can be calculated following the general procedure outlined in [26] to give

$$P_{n1}(q') = \frac{2^8 n^7 q'^2 [n^2(3q'^2+1)-1)}{3[(n^2q'^2+1)^2 + 2n^2(n^2q'^2-1)+n^4]^3} \times \left(\frac{n^2q'^2 + (n-1)^2}{n^2q'^2 + (n+1)^2} \right)^n, \tag{23}$$

where $q'=q/Z$ is the momentum boost scaled by the nuclear charge Z. This function exhibits a maximum which is located at increasing q' as n increases. For $n=2$ the maximum is at $q' \approx 0.75$ a.u., and as $n \to \infty$ it shifts to $q' \approx 0.9$ a.u. From Fig. 5(b) one sees that this is the q region in which the ionization probability maximizes. As seen in Fig. 5(a), this also coincides with the rapid increase of ionization probability. In Fig. 5 the probabilities obtained from a DVR calculation using both rectangular and sinusoidal pulses are shown also. In all cases the exact DVR results for both pulse forms agree perfectly with the FMA results on the scale of Fig. 5.

The fact that for large enough q all atoms are 100% ionized after a half-cycle pulse can be used to advantage to derive approximate analytic expressions for initial-state

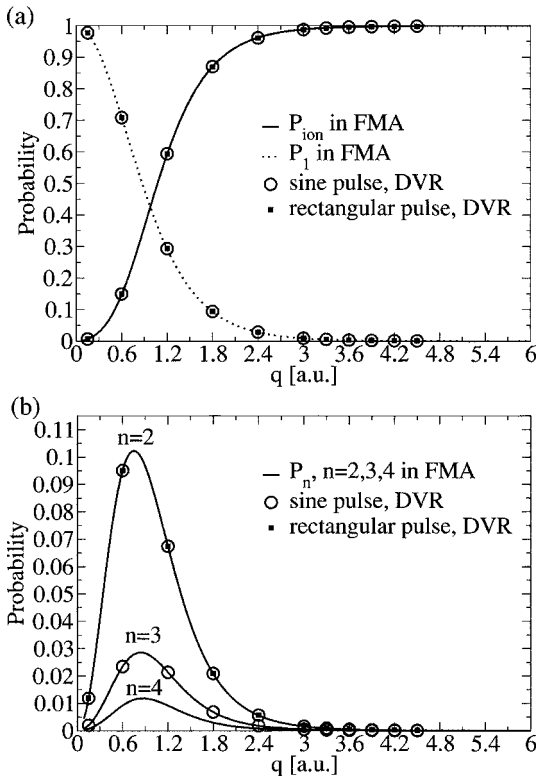

FIG. 5. Probability of (a) ionization and population of the $Z=1$ ground state, and (b) population of the $n=2,3,4$ shell, after one half-cycle pulse with $\tau=0.3$ a.u. The FMA is compared to the numerical calculation (DVR) for both sinusoidal and rectangular pulses.

populations after N complete cycles of the field. We begin with $N=1$ where Eq. (22) reduces to

$$a_{fi}(1) = \langle \phi_f | e^{i\mathbf{q}\cdot\mathbf{r}} e^{-i\hat{H}_0\tau} e^{-i\mathbf{q}\cdot\mathbf{r}} | \phi_i \rangle. \tag{24}$$

If we introduce a complete set of hydrogen eigenstates as intermediate states then Eq. (24) becomes

$$a_{fi}(1) = \sum_{n=1}^{\infty} \langle \phi_f | \exp(i\mathbf{q}\cdot\mathbf{r}) | \phi_n \rangle \langle \phi_n | \exp(-i\mathbf{q}\cdot\mathbf{r}) | \phi_i \rangle \times \exp(-iE_n\tau) + \int d^3\mathbf{k} \langle \phi_f | \exp(i\mathbf{q}\cdot\mathbf{r}) | \phi_\mathbf{k} \rangle \langle \phi_\mathbf{k} | \times \exp(-i\mathbf{q}\cdot\mathbf{r}) | \phi_i \rangle \exp\left(-i\frac{k^2}{2}\tau\right). \tag{25}$$

In Fig. 6(a) the full circles show the decreasing probability of being in the ground state after a one-cycle pulse as q is increased. At $q\sim 3$ a.u. this amounts to around 80%. However this cannot be assigned to population which has *remained* in the ground state. In Fig. 6(a) is also shown (empty circles) the probability of ionization after a half-cycle pulse, obtained by numerical DVR calculation, which is in perfect agreement with the FMA half-cycle result (dotted line). For $q\sim 3$ a.u. this amounts to almost 100%. Hence one concludes that on the first half cycle all electrons are ionized and 80% of them are returned to the ground state by the second half cycle. This extremely large probability of recombination corresponds then to "Rabi flopping" on the continuum, as was shown explicitly in I and will be illustrated more strikingly below. That this interpretation is correct is also to be seen from the dashed line in Fig. 6(a). This denotes the final ground-state population emanating from the electrons in the continuum after a half cycle. Above $q\sim 2.5$ a.u. the final population of the ground state has come exclusively from recombination of continuum electrons. Since this is so, we can see that, above $q\sim 2.5$ a.u., one can neglect the contribution of all bound states as intermediate states in Eq. (25). Then, if we assume that the discrete initial and the final states are identical, the probability of population of the initial state after the second δ pulse is

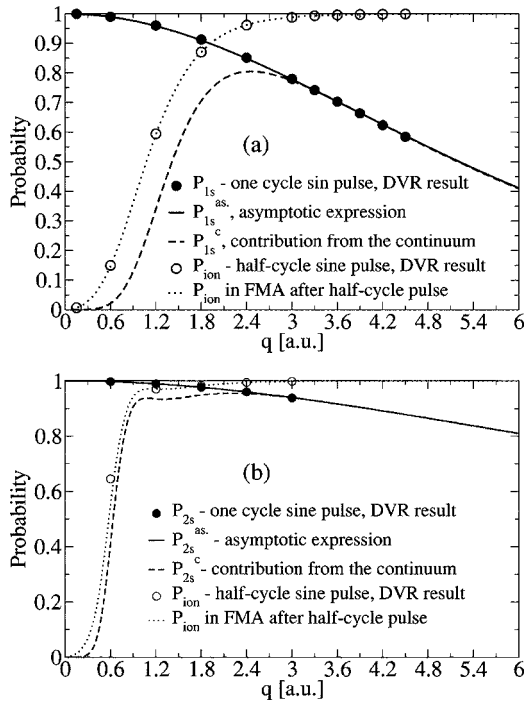

FIG. 6. (a) The probability P_1 of occupation of the ground state after a one-cycle sine pulse with $\tau=0.3$ a.u. and the probability P_{ion} of occupation of continuum states after a half cycle. (b) The same probabilities for the $2s$ initial state. In both cases $Z=1$.

$$P_{ii} = \left| \int d^3\mathbf{k} | \langle \phi_\mathbf{k} | \exp(-i\mathbf{q}\cdot\mathbf{r}) | \phi_i \rangle |^2 \exp\left(-i\frac{k^2}{2}\tau\right) \right|^2. \tag{26}$$

In the case when the initial state is the ground state the above expression reduces to (denoting P_{ii} simply as P_1)

$$P_1 = \left| \int I(k') \exp\left(-i\frac{k'^2}{2}\tau'\right) dk' \right|^2, \tag{27}$$

where the scaling $k'=k/Z$, $\tau'=\tau Z^2$ is used and the function $I(k')$ is given by [26]

$$I(k') = \frac{2^8 q'^2 k' (3q'^2 + k'^2 + 1) \exp\{-(2/k')\tan^{-1}[2k'/(q'^2 - k'^2 + 1)]\}}{3[(q'-k')^2+1]^3[(q'+k')^2+1]^3[1-\exp(2\pi/k')]}. \tag{28}$$

In the limit $q'\to\infty$, one obtains the following asymptote:

$$I(k') \approx \frac{8}{3\pi} \frac{1}{[1+(q'-k')^2]^3}. \tag{29}$$

If we linearize the k' dependence of the energy phase factor in Eq. (27), i.e.,

$$\exp\left(-i\frac{k'^2}{2}\tau'\right) \approx \exp[-i(k'-q')q'\tau'] \exp\left(-i\frac{q'^2}{2}\tau'\right), \tag{30}$$

then one can integrate the above asymptotic expression, and the ground-state occupation probability assumes the simple analytic form

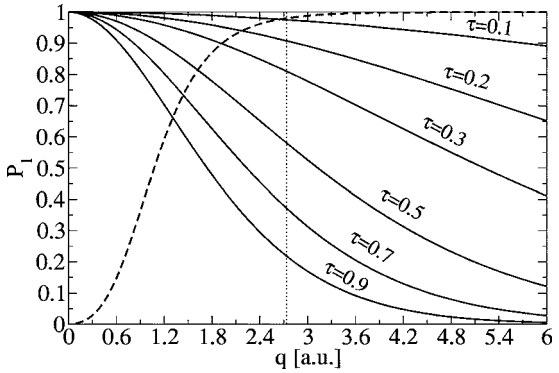

FIG. 7. Full lines: ground-state occupation probability after a one-cycle sine pulse for different τ's according to the asymptotic formula (31). Dashed line: probability of ionization after the first half cycle in the FMA. Results are plotted for $Z=1$.

$$P_1^{as} = \exp(-2q'\tau')\left(1 + q'\tau' + \frac{(q'\tau')^2}{3}\right)^2. \qquad (31)$$

From Fig. 6(a) one sees that this analytic form for P_1 (denoted by the continuous line) agrees with the numerical DVR result for $q>3$ a.u.. However, although the approximation that only continuum states function as intermediate states is not justified for $q<2.5$ a.u., the analytic asymptote is valid all the way down to $q=0$. This is a happy accident caused by the fact that expression (31) has the correct $q=0$ value and the probability is smooth and monotonic in q.

The monotonic decrease of P_1 as a function of q is shown in Fig. 7 for various values of τ. Also shown is the ionization probability after a half cycle, which in the FMA depends only on q and not on τ. One sees that for $\tau=0.1$ a.u. even at $q=6$ a.u., 90% of the population returns to the ground state. Recombination at the 80% level is still achieved at $q=0.9$ a.u. for $\tau=0.9$ a.u. The qualitative behavior of the curves of Fig. 7 is readily understood in the region $q>3$ a.u. The first pulse puts electrons in the continuum centered around $k=q$. Hence the electrons have time τ to diffuse away before the recombining pulse occurs. The larger is q and the longer is τ, the more electrons will diffuse out of the ground-state wave packet whose initial momentum-space coherent shape is unchanged by the impulsive transfer of momentum. The more electrons diffuse away the fewer are available to be recombined by the second half of the one-cycle pulse.

Calculations have been performed also for initial $2s$ and $2p$ states. The results for $2s$, for the same q and τ values shown in Fig. 6(a) for $1s$, are given in Fig. 6(b). One notes that already for $q>1$ a.u., 100% ionization is caused by the first half-cycle pulse. Compared to the ground state, this lower value of q to achieve ionization is simply due to the lower binding energy. The minimum "momentum kick" to be given to a bound electron to ionize is given by $\frac{1}{2}q^2 = \frac{1}{2}Z^2/n^2$, i.e., by $q=Z/n$. This gives $q=1$ a.u. for the $n=1$ ground state of hydrogen and $q=0.5$ a.u. for $n=2$. This is in rough agreement with the onset of ionization shown in Fig. 6. One also notes, from the exact DVR results for P_1 after a one-cycle $\tau=0.3$ a.u. pulse shown in Fig. 6(b), that now at $q=3$ a.u., 90% of the ionized electrons recombine. For a $1s$ initial state this value is only 80%. From the arguments given above one might expect that the number of electrons escaping before recombination depends only on q and τ. However the reduction for $2s$ is readily explicable. The width of the continuum momentum distribution (the ground-state distribution boosted by momentum $\mathbf{q}$) is proportional to Z/n. Clearly it is the high-momentum electrons that diffuse away fastest and, as the momentum spread of $2s$ is a factor of 2 smaller than for $1s$, there is less diffusion out of the coherent momentum wave packet and therefore a higher recombination probability.

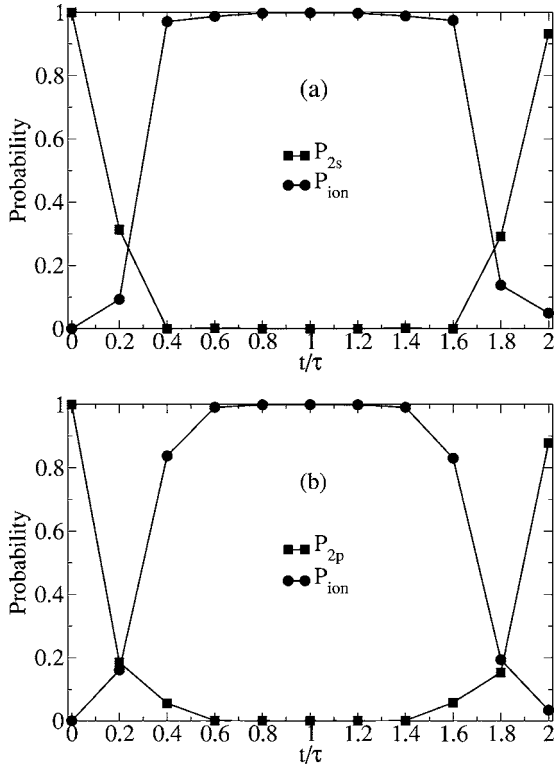

FIG. 8. Recombination into the initial states (a) $2s$ and (b) $2p$ under the influence of a short, one-cycle pulse; plots for $Z=1$.

Using a similar procedure as led to Eq. (31) (see the Appendix), one can obtain an asymptotic expression for the population of the 2s state after a full-cycle pulse, when one starts from the $2s$ state. This is given by

$$P_{2s}^{as} = \exp(-q'\tau')\left(1 + \frac{q'\tau'}{2} + \frac{(q'\tau')^2}{12} + \frac{(q'\tau')^4}{240}\right)^2. \qquad (32)$$

This curve is shown on Fig. 6(b) as a continuous line and, as in the $1s$ case, is in perfect agreement with DVR results, not only for asymptotically large q but over the complete range of q values.

In paper I we presented the time development of the occupation probability of initial $1s$ and continuum states (Fig. 5 of that paper) which showed explicitly that in a single full-cycle pulse, almost 100% ionization occurs after a half cycle and ~80% recombination after a full cycle, i.e., a kind of Rabi flopping on the continuum occurs. In Fig. 8 we show the same plots for an initial $2s$ or $2p$ state, for the same q and τ values. In this case one notes a rapid full depletion of the

initial state into the continuum and then 90% repopulation of the initial state. One might question why repopulation occurs almost exclusively into the original initial state, since after 100% ionization all bound states are unoccupied. Presumably, the answer simply lies in the fact that the initial bound-state momentum wave packet $\tilde{\phi}_i(\mathbf{p})$ is transferred unaltered to $\tilde{\phi}_i(\mathbf{p}+\mathbf{q})$ on the first half cycle. If there is no appreciable spreading of this packet before the second half cycle, which provides momentum $\mathbf{q}$, then the whole wave packet becomes $\tilde{\phi}_i(\mathbf{p})$ again, which has zero overlap with states other than the initial state i.

Even more interesting is a train of N pulses. The TDSE Eq. (5) has been solved exactly numerically to obtain the initial-state and continuum populations as a function of time and the results are presented for an initial $1s$ state, in Fig. 10 for a two-cycle train and in Fig. 11 for a five-cycle train of pulses. The modified FMA for the transition amplitude is given by Eq. (22) and represented symbolically in Fig. 9 by a train of alternating δ pulses. A negative amplitude represents a pulse that returns the continuum electron to the initial state, where it remains until a positive amplitude pulse puts it back in the continuum after a lapse time τ. During this time the time-dependent wave function simply acquires a constant phase $\exp(-iE_i\tau)$. For N pulses this is a phase $\exp(-iE_iN\tau)$ which does not contribute to $P_{fi}=|a_{fi}|^2$ from Eq. (22). This implies that in Eq. (22) one can put

$$e^{-i\mathbf{q}\cdot\mathbf{r}}e^{-i\hat{H}_0\tau}e^{i\mathbf{q}\cdot\mathbf{r}} = 1 \tag{33}$$

to give, as simplification,

$$a_{fi}(N) = \langle\phi_f|e^{i\mathbf{q}\cdot\mathbf{r}}e^{-i\hat{H}_0N\tau}e^{-i\mathbf{q}\cdot\mathbf{r}}|\phi_i\rangle. \tag{34}$$

That is, a train of N cycles is equivalent, in this approximation to the modified FMA of Eq. (22), to a one-cycle pulse with a delay of $N\tau$ between half cycles. This approximation is shown symbolically in Fig. 9(c) with the equivalent one-cycle pulse $F_1(t)$. Hence the analytic forms [Eqs. (31) and (32)] for the population of the initial state after one cycle can be applied for N cycles, simply by replacing τ' by $N\tau'$. The results of this approximation are shown also on Figs. 10 and 11 after each cycle and are in very good (and sometimes perfect) agreement with the accurate DVR results.

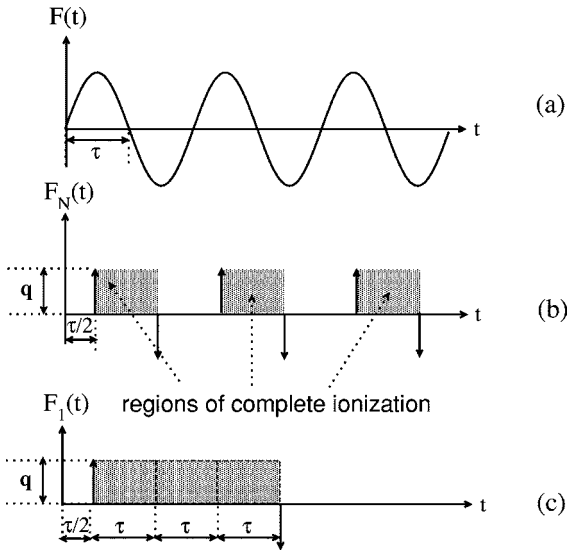

FIG. 9. (a) Electric field time dependence $[F(t)]$. (b) A train of alternating δ pulses modeling the electric field $[F_N(t)]$. Shaded regions denote the time intervals in which the population is entirely in the continuum. (c) The equivalent one-cycle pulse $[F_1(t)]$.

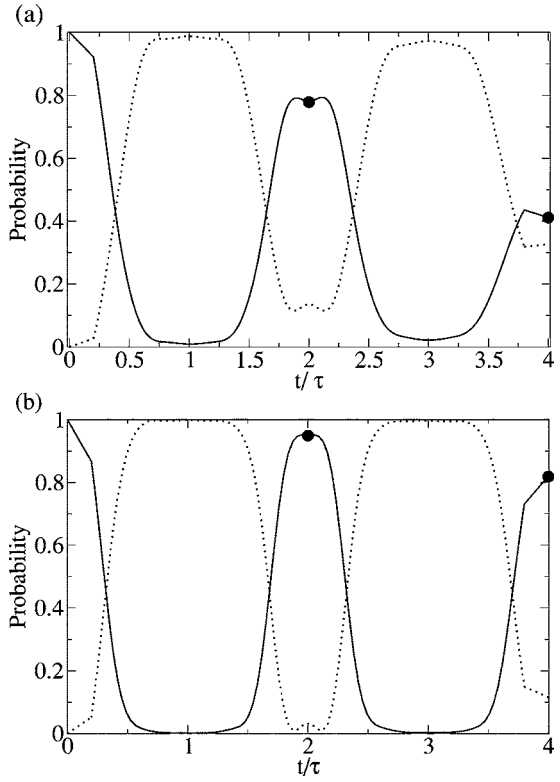

FIG. 10. Full lines: $Z=1$ ground-state occupation probability as a function of time. Pulses with (a) $q=3$ a.u., $\tau=0.3$ a.u. and (b) $q=4$ a.u. $\tau=0.1$ a.u. Dotted lines: probability of ionization. Full circles: analytic asymptotic expression for the ground-state occupation probability after N full cycles ($N=1-2$).

Figure 10 illustrates the Rabi flopping from the ground state for relatively large q values and for $\tau=0.3$ and 0.1 a.u. and a total duration of two cycles, i.e., $t=4\tau$. One sees clearly again that for larger q and shorter τ the Rabi flopping is less damped. The N-cycle results are shown in Fig. 11 and illustrate that the rate of decrease of P_1 as $q\tau$ increases is quite strong i.e. as expected from Eq. (34), one needs $q\tau \ll 1$ a.u. but also $q>1$ a.u. and therefore $\tau \ll 1$ a.u. to achieve significant Rabi flopping over a few cycles. The N-cycle formula (34) agrees also for the $2s$ state, as we have explicitly checked by a numerical calculation and as is illustrated in Fig. 12.

V. CONCLUSIONS

We have examined the ionization of a hydrogenic atom from the $n=1$ and 2 states by short laser pulses consisting of a half cycle up to the order of five full cycles. We have compared and contrasted three levels of approximation: (1) the fully numerical propagation of the time-dependent wave

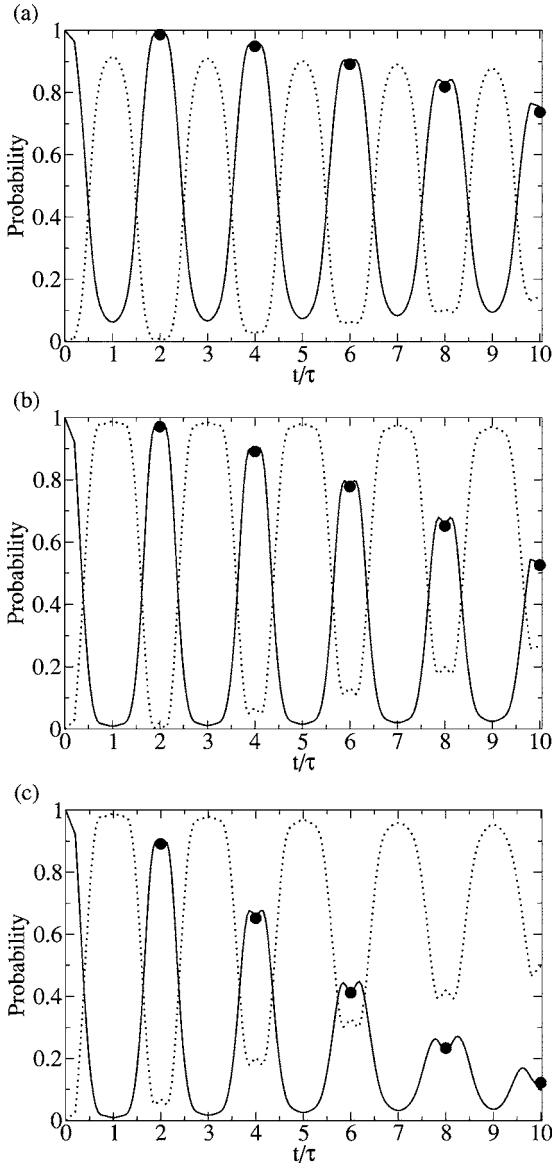

FIG. 11. Full lines: $Z=1$ ground-state occupation probability as a function of time. Pulses with (a) $q=2$ a.u., $\tau=0.1$ a.u., (b) $q=3$ a.u., $\tau=0.1$ a.u., and (c) $q=3$ a.u., $\tau=0.2$ a.u. Dotted lines: probability of ionization. Full circles: analytic asymptotic expression for the ground-state occupation probability after N cycles ($N=1-5$).

function, (2) the FMA, appropriate for short pulses of arbitrary field strength, and (3) the FPA, appropriate for weak pulses of arbitrary duration. In the case of the FPA, analytic formulas for rectangular and sinusoidal pulses consisting of m half cycles have been obtained. For a finite number of pulses the energy distribution shows considerable structure, peaking at zero electron emission energy for $\tau<1$ a.u. However, when $\tau>1$ a.u. or the number m of half cycles tends to infinity, a peak appears in the energy spectrum corresponding to the energy conservation condition for one-photon absorption, i.e., at electron energy $E=-|E_i|+\pi/\tau$. For a small number of cycles, beginning with a half cycle $N=1/2$, we have shown that the population of excited and continuum states, though small, exhibits oscillations in time, with a maximum for odd m and a minimum for even m. Particularly for low-

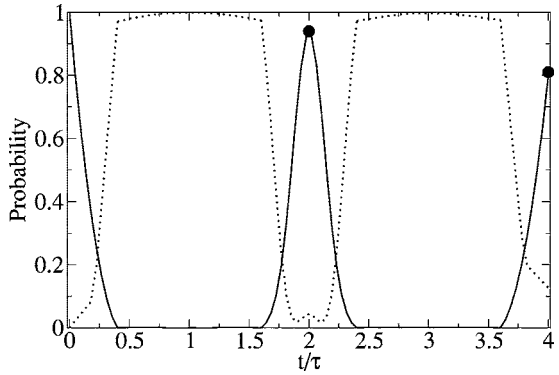

FIG. 12. Full line: $2s$-state occupation probability as a function of time for a pulse with $q=3$ a.u., $\tau=0.3$ a.u., and for $Z=1$. Dotted line: probability of ionization. Full circles: analytic asymptotic expression for the initial-state occupation probability after N cycles ($N=1-2$).

energy electron emission, in the case of $m=4$, the ionization probability shows strong dependence on the phase of the pulse with respect to the maximum of the carrier envelope.

In the FMA for $\tau\ll 1$ a.u. we have shown that the ionization probability is independent of the precise shape of the pulse and can be represented as a train of alternating δ pulses separated by a time τ. The transition amplitude after each half cycle is decided by the momentum boost operator $\exp(i\mathbf{q}\cdot\mathbf{r})$, where $\mathbf{q}$ is the momentum transferred from field to atom. The analogy here to the scattering of fast charged particles has been emphasised. For small $\mathbf{q}$, such that $\mathbf{q}\cdot\mathbf{r}\ll 1$ for all relevant r values, only the dipole term is important and this sudden approximation gives a $\cos^2\theta$ angular distribution, as in the FPA, and an energy distribution peaking at $E=0$ for a single half-cycle pulse. However, as q increases the angular distribution becomes more and more peaked in the field direction and the energy shows a maximum at the "binary peak" corresponding to transfer of all momentum to the electron with the nucleus acting as spectator. In the FMA the angular distribution becomes more and more peaked along the field direction as the momentum transfer is increased (see Fig. 4).

For $N=1/2$, all probability is transferred to the continuum when q exceeds approximately 2 a.u. for the $1s$ state and 1 a.u. for the $2s$ state. For these q values, for $N=1$ almost all probability returns to the initial state, a process akin to Rabi flopping from the continuum. For the $n=2$ state, this process is even more pronounced. So long as $\tau\ll 1$ a.u. this flopping continues for several cycles before the initial state is appreciably depopulated.

Under the approximation that, for N equal to a half integer, all population previously in the initial state is transferred to the continuum and in the subsequent half cycle is transferred back to the initial state, a simple analytic form has been obtained for the population of the initial state after N cycles. For both $1s$ and $2s$ as initial state this formula is in excellent agreement with the exact DVR result.

The calculations have been carried out on the hydrogen atom so that the numerical results can be obtained without further approximation and the analytic results in closed form. However, the key results in short-pulse ionization depend

only on the facts that the orbital time in the initial state is much longer than the pulse duration τ and that the momentum transfer q is much larger than the width of the momentum distribution of the initial state. For hydrogenic atoms this width is Z/n or $|2E_i|^{1/2}$ where $|E_i|$ is the initial-state binding energy. Hence for nonhydrogenic atoms equivalent results should be obtained with qualitatively similar character if $q\tau$ in atomic units is scaled by a factor $|2E_i|^{1/2}$.

APPENDIX

In order to derive the asymptotic expression (32) we start from the explicit expression for the matrix element $I(k')=k'^2\int|\langle\phi_{\mathbf{k}'}|\exp(-i\mathbf{q}'\cdot\mathbf{r}')|\phi_{2s}\rangle|^2 d\hat{\mathbf{k}}'$ given in [26], i.e.,

$$I=\frac{2^5 q'^2 k' \exp\{-(2/k')\tan^{-1}[k'/(q'^2-k'^2+1/4)]\}}{3[1-\exp(2\pi/k')][(q'-k')^2+1/4]^5[(q'+k')^2+1/4]^5}\times\left[3q'^{10}+(8-11k'^2)q'^8+\left(\frac{41}{8}+18k'^2+14k'^4\right)q'^6+\left(\frac{5}{16}-\frac{31}{8}k'^2-10k'^4-6k'^6\right)q'^4+\left(\frac{47}{320}-\frac{47}{80}k'^2-\frac{7}{4}k'^4-k'^6\right)\left(\frac{1}{4}+k'^2\right)q'^2+(1+k'^2)\left(\frac{1}{4}+k'^2\right)^4\right], \tag{A1}$$

where we use the scaled quantities $\mathbf{k}'=\mathbf{k}/Z$, $\mathbf{q}'=\mathbf{q}/Z$, $\mathbf{r}'=Z\mathbf{r}$. From the fact that in the limit of $q'\to\infty$ there is a well-defined peak in Eq. (A1) at $k'=q'$, we can factor the expression as follows:

$$I=f(k',q')\times g(k',q'), \tag{A2}$$

where $f(k',q')=[(q'-k')^2+1/4]^{-5}$ is the part of the expression (A1) that defines the peak at $k'=q'$. Next, by developing $g(k',q')$ in a Taylor series with respect to k' at the point $k'=q'$ and subsequently taking the limit $q'\to\infty$ for the coefficients, one obtains,

$$\lim_{q'\to\infty} g(k',q')=\frac{1}{120\pi}-\frac{(k'-q')^2}{12\pi}+\frac{(k'-q')^4}{3\pi}. \tag{A3}$$

Inserting (A3) into (A2), we get an asymptotic expression for $I(k')$. Using the linearization (30), the integral (27) reduces to

$$\int_{-\infty}^{\infty}\frac{\exp(-iq'\tau' u)(1-10u^2+40u^4)}{120\pi(u^2+1/4)^5}du. \tag{A4}$$

Integrating Eq. (A4) and taking the squared modulus of the result one obtains the asymptotic expression (32).

[1] T. Brabec and F. Krausz, Rev. Mod. Phys. **72**, 545 (2000).
[2] V. Ayvazyan *et al.*, Phys. Rev. Lett. **88**, 104802 (2002).
[3] H. Walbnitz *et al.*, Nature (London) **420**, 482 (2002).
[4] M. Hentschel *et al.*, Nature (London) **414**, 509 (2001).
[5] A. Baltuška *et al.*, Nature (London) **421**, 611 (2003)
[6] R. Kienberger *et al.*, Nature (London) **427**, 817 (2004).
[7] R. López-Martinez *et al.*, Phys. Rev. Lett. **94**, 033001 (2005).
[8] G. G. Paulus *et al.*, Nature (London) **414**, 182 (2001).
[9] D. B. Milošević, G. G. Paulus, and W. Becker, Phys. Rev. Lett. **89**, 153001 (2002).
[10] D. B. Milošević, G. G. Paulus, and W. Becker, Laser Phys. Lett. **1**, 93 (2004).
[11] G. Duchateau, E. Cormier, and R. Gayet, Eur. Phys. J. D **11**, 191 (2000).
[12] A. Wetzels *et al.*, Phys. Rev. Lett. **89**, 273003 (2002).
[13] J. G. Zeibel and R. R. Jones, Phys. Rev. A **68**, 023410 (2003).
[14] D. G. Arbó, C. O. Reinhold, and J. Burgdörfer, Phys. Rev. A **69**, 023409 (2004).
[15] C. O. Reinhold, M. Melles, H. Shao, and J. Burgdörfer, J. Phys. B **26**, L659 (1993).
[16] P. Krstic and Y. Hahn, Phys. Rev. A **50**, 4629 (1994).
[17] A. Bugacov, B. Piraux, M. Pont, and R. Shakeshaft, Phys. Rev. A **51**, 1490 (1995).
[18] D. Dimitrovski, E. A. Solov'ev, and J. S. Briggs, Phys. Rev. Lett. **93**, 083003 (2004).
[19] D. Dimitrovski, T. P. Grozdanov, E. A. Solov'ev, and J. S. Briggs, J. Phys. B **36**, 1351 (2003).
[20] W. Magnus, Commun. Pure Appl. Math. **7**, 649 (1954).
[21] P. Pechukas and J. C. Light, J. Chem. Phys. **44**, 3897 (1966).
[22] L. I. Schiff, *Quantum Mechanics*, 3rd ed. (McGraw-Hill, New York, 1968), p. 292.
[23] A. M. Dykhne and D. L. Yudin, Sov. Phys. Usp. **21**, 549 (1978).
[24] V. I. Matveev and E. V. Ivanova, Russ. Phys. J. **46**, 386 (2003).
[25] J. Itatani, H. Niikura, and P. B. Corkum, Phys. Scr., T **110**, 112 (2004).
[26] A. R. Holt, J. Phys. B **2**, 1209 (1969).
[27] H. A. Bethe, Ann. Phys. **5**, 325 (1930).
[28] Dž Belkić, J. Phys. B **17**, 3629 (1984).
[29] P. L. Shkolnikov, A. E. Kaplan, and S. F. Straub, Phys. Rev. A **59**, 490 (1999).
[30] A. D. Bandrauk and H. Shen, Chem. Phys. Lett. **176**, 428 (1991).
[31] H. Wiedemann, J. Mostowski, and F. Haake, Phys. Rev. A **49**, 1171 (1994).